JOINT INSTITUTE FOR NUCLEAR RESEARCH
Frank Laboratory of Neutron Physics

FINAL REPORT ON THE SUMMER STUDENT PROGRAM

The study of intramolecular hydrogen bonds in bilirubin by spectroscopic methods

Supervisor:
Prof. Dr. Sc. Aleksander Filarowski

Student:
Mikhail Kostin, Russia
Saint Petersburg State University, Faculty of Physics

Participation period:
August 01 – August 31

Dubna, 2021

Contents

Annotation

This work contains the results of research carried out during my Summer Student Program at Joint Institute for Nuclear Research. The unique experimental equipment of the Institute, cooperation with specialists and the possibility of obtaining experimental data using this equipment allowed us to conduct a study using the method of incoherent inelastic neutron scattering (IINS). The main object of research during Student Program is hydrogen bond in bilirubin. Bilirubin is found in catabolic process in organism, is a cellular antioxidant, bilirubin concentration in the blood is used to diagnose certain diseases. The use of IINS method in conjunction with other spectroscopic methods (IR spectroscopy and Raman spectroscopy), and quantum-chemical calculations, provide the most complete information about vibrational modes. Due to its special sensitivity to hydrogen atom and isotope substitution, and the possibility of recording spectra in the region of low wavenumbers, IINS method is useful tool to obtain characteristics of hydrogen bonds that are inaccessible by other spectral methods.

Hydrogen bonding

Among all noncovalent interactions, hydrogen bonds are important in chemistry [1,2], biology [3,4,5,6], materials science [7].

The presence of a hydrogen bond affects macroscopic parameters: boiling point and melting point of substances, the ability to enter into chemical reactions, polymerization, etc.

The definition of hydrogen bonds is given by IUPAC and is expressed as follows [8]: *The hydrogen bond is an attractive interaction between a hydrogen atom from a molecule or a molecular fragment X–H in which X is more electronegative than H, and an atom or a group of atoms in the same or a different molecule, in which there is evidence of bond formation*.

Hydrogen bond is designated as follows: X–H···Y–Z. The three dots represent the hydrogen bond. Because of their widespread occurrence and extreme importance, hydrogen bonds are the subject of detailed study. The data on hydrogen bonds accumulated during the study allow them to be classified into separate groups, for example:

- Intramolecular or intermolecular bonds
- Hydrogen bonds with or without proton transfer from atom X to atom Y.

The most important characteristics of hydrogen bond are geometry and strength. The hydrogen bond lengths (r_1 and r_2), the bond angles (α and β), and bond strength (ΔE) are most often used to describe the properties of the hydrogen bond (Fig. 1). The strength of hydrogen bonds is much less than the strength of covalent bonds and ranges from 0–4 kcal/mol for the weakest hydrogen bonds and up to 15–45 kcal/mol for the strongest hydrogen bonds [9].

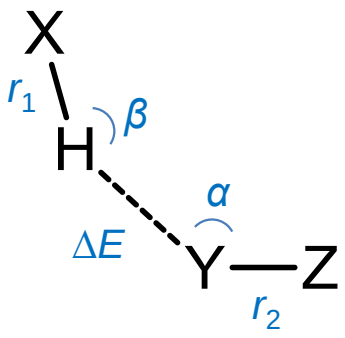

Fig. 1. The most commonly used parameters to describe hydrogen bonds

A set of methods is used to diagnose and describe hydrogen bonds. The most commonly used methods are:

- NMR Spectroscopy
- IR Spectroscopy
- Raman Spectroscopy
- Neutron scattering
- Quantum mechanical calculations

The choice of the method is due to the choice of hydrogen bonds parameters that need to be determined, and the properties of studied chemical compounds. A brief description of each of these methods as applied to hydrogen bonds is presented in the next section.

Methods for the study of hydrogen bonds

NMR

NMR method is based on the phenomenon of resonant absorption or emission of electromagnetic energy by a compound containing nuclei with nonzero spin in an external magnetic field, at frequency ν, due to the reorientation of nuclear magnetic moments. Depending on the environment, the same nuclei show different NMR signals.

NMR method provides information on molecular structure of chemical compounds, allows one to study dynamic processes in a sample, such as the rates of chemical reactions and the magnitude of energy barriers to intramolecular rotation.

In addition NMR method makes it possible to identify hydrogen bonds in compounds. There are several approaches for detecting and describing hydrogen bond properties. Most often, these approaches are based on a change in nuclear chemical shift during the formation of hydrogen bond [10,11]. Such a nucleus can be the nucleus of hydrogen atom participating in hydrogen bond formation or another nucleus that is sensitive to the formation of hydrogen bond and is located near this bond, for example, the nucleus of phosphorus, nitrogen, etc. [12,13,14].

Quantum chemical calculations

Calculation methods are based on the application of quantum mechanics to chemical systems. Understanding the structure of a substance and its properties based on the Schrödinger equation is the main task of computational methods. There are a number of methods for conducting quantum chemical research. Many of the methods assume that the nuclei remain stationary relative to electrons motion (Born-Oppenheimer approximation). The choice of theory level for carrying out calculations is determined by the size of molecular system, atoms numbers and computing power. Quantum chemistry methods make it possible to find the positions of atoms in a system and predict NMR, IR and Raman spectra for this compound. Multielectron systems can be described in terms of electron density instead of wave functions. This approach is the basis for density functional theory (DFT), which is widely recognized due to the good ratio of calculation speed and accuracy of results. The calculation speed depends on level of theory and the number of atoms in investigating system.

Quantum-chemical calculations are actively used to study hydrogen-bonded systems. It is possible to investigate hydrogen bond geometry (lengths and angles), bond strength, vibration frequency of atoms involved in hydrogen bond formation (IR spectra) and chemical shifts of individual atoms (NMR spectra). The calculated results obtained can be compared with experimental data [15,16,17]. Often, based on quantum chemical calculations, it is possible to assign signals in experimental spectra.

IR Spectroscopy

This is a branch of spectroscopy that studies the interaction of infrared radiation with material. When infrared radiation is passed through a material, vibrational movements of molecules or their individual fragments are excited. In this case, a weakening of the intensity of the light transmitted through the sample is observed. However, absorption does not occur in entire spectrum of incident radiation, but only at those wavelengths, the energy of which corresponds to excitation energies of vibrations in the molecules. Consequently, the wavelengths (or frequencies) at which the maximum absorption of IR radiation is observed indicate the presence of certain functional groups and other fragments in the sample molecules, which is widely used in various fields of chemistry to determine the structure of compounds.

Interaction with hydrogen bonds leads to significant changes in infrared spectrum, for example, to a frequency shift by tens and in some cases hundreds of cm^{-1} and an increase in IR radiation intensity for bands related to vibrational modes of functional groups directly involved in hydrogen bond formation [18,19,20]. IR is the primary method for hydrogen bond detection in liquid, solid and gas phase.

Raman Spectroscopy

Raman spectroscopy is based on inelastic photon scattering, known as Raman scattering. Raman spectroscopy is commonly used in chemistry to produce a structural fingerprint from which molecules can be identified. Laser light interacts with molecular vibrations, phonons (quantum of vibrational motion of crystal atoms) or other excitations in the system, as a result of which the energy of laser photons is shifted up or down. The energy shift provides information about vibrational modes in the system.

Raman effect is based on the interaction between electron cloud of the compound and external electric field of monochromatic light, which can create an induced dipole moment inside the molecule based on its polarizability. IR spectroscopy provides information on the change in the derivative of electric dipole moment under the influence of external radiation. Therefore, transitions that cannot be active in infrared range can be analyzed using Raman spectroscopy. Both IR and Raman methods are suitable for the analysis of solids, powders, liquids, gels, suspensions and gases.

Hydrogen bond can be detected by Raman spectroscopy methods by changing vibration frequency of individual groups in the spectra.

Neutron scattering

Neutrons scattering by matter can be considered as a special type of spectroscopy. This method investigates the interaction of neutrons with matter. Neutrons have a number of specific properties that make them useful for condensed matter studies [21]:

- Neutrons are neutral particles. They have a high penetrating power, do not destroy test substance, and are suitable for examining samples at both very low and very high temperatures.
- The wavelengths of neutrons are similar to atomic distances and are in the range from 10^{-6} Å to 10^{3} Å. Therefore, information about the structure of a substance can be obtained.
- The values of thermal neutrons energy are comparable to elementary excitations energies in solids. Therefore, using neutrons, it is possible to study molecular vibrations, lattice excitations and the dynamics of atomic motion.
- Neutrons interact with nuclei (as opposed to X-rays or electrons, which interact with an electron cloud). Neutrons are very sensitive to light atoms such as hydrogen (hydrogen has the largest scattering cross section for neutrons). The hydrogen atom is difficult to detect with X-rays because hydrogen bonds often have less than one surrounding electron.
- Neutron scattering techniques are used to distinguish between adjacent elements in the periodic table, such as manganese, iron and chromium. Isotopic substitution can also be investigated. The most famous example is the study of the replacement of hydrogen by deuterium in certain molecules or functional groups.

There are several types of neutron scattering in matter. The information that can be obtained from a neutron scattering experiment depends on which type of neutron scattering is observed.

Scattering can be elastic or inelastic, coherent and incoherent. Thus, there are four types of neutron scattering in matter: elastic coherent, elastic incoherent, inelastic coherent and inelastic incoherent scattering.

In the case of elastic scattering, the neutron energy does not change during scattering. A neutron beam hits on a stationary target, as a result of which the neutron energy does not change, but the direction of neutron movement changes.

With inelastic scattering, neutron energy decreases or increases. This is due to vibrations of nuclei, which can exchange energy with neutrons.

Scattering is coherent if it includes wave interference. Neutrons scattered from different nuclei interfere with each other, i.e. neutrons interact with the substance as with one whole. Therefore, this type of scattering provides information about the structure of matter.

Conversely, if neutrons are scattered by different nuclei without interference, then the scattering is incoherent.

Elastic scattering (diffraction) provides information about the position of atoms (molecules) and allows one to study the structure of a compound.

Inelastic neutron scattering is used to study atomic (molecular) dynamics, i.e. allows us to study the interactions of atoms (molecules). This method provides valuable information on elementary excitations due to translational, vibrational and rotational degrees of freedom of atoms or molecules.

In addition, inelastic incoherent neutron scattering (IINS) method [22] is used to determine the vibration frequencies in molecules, which can exhibit weak intensity in IR and Raman spectra. The combination of three spectroscopic methods (IR spectroscopy, Raman spectroscopy and IINS) provides the most comprehensive information on vibrational processes in studied compounds [23].

Theoretical framework of neutron scattering

The neutron has the properties of a particle and a wave at the same time. Neutrons interact with atomic nuclei via very short range (~ fm) forces. The scattering of neutrons can be described mathematically [24]. The main characteristic of the beam incident on the sample is the flux Φ, which is equal to the number of incident neutrons per cm per second. To describe the scattered flux, the scattering cross section is used, which is the total number of neutrons scattered per second (N) relative to the flux Φ, i.e.:

$$\sigma = \frac{N}{\Phi} \qquad (1)$$

To describe the spatial angular distribution of scattered neutrons, the differential scattering cross section is used:

$$\frac{\mathrm{d}\sigma}{\mathrm{d}\Omega} = \frac{N(d\Omega)}{\Phi \mathrm{d}\Omega} \qquad (2)$$

In equation (2), the quantity $N(d\Omega)$ is the number of neutrons scattered per second into $d\Omega$.

In the case of inelastic scattering, equation (3) is used, which takes into account the energy distribution of scattered neutrons. Parameter $N(d\Omega, \mathrm{dE})$ is the number of neutrons scattered per second into $d\Omega$ and dE.

$$\frac{\mathrm{d}^2\sigma}{\mathrm{d}\Omega \mathrm{dE}} = \frac{N(d\Omega, \mathrm{dE})}{\Phi \mathrm{d}\Omega \mathrm{dE}} \qquad (3)$$

The simplest case is the scattering of a neutron on one stationary atom (Fig. 2). The energy of the neutron is too small to change the energy of the nucleus, and the neutron cannot transfer kinetic energy to fixed nucleus, therefore the scattering is elastic. A neutron moving along the X axis is described by the wave function ψ_0:

$$\psi_0 = e^{ikx} \qquad (4)$$

After scattering, the wave function takes the form:

$$\psi_{scat} = \frac{-b}{r} e^{ikr} \qquad (5)$$

The parameter *b* is scattering length, which depends on the isotope and can be positive or negative. The velocity of neutron before and after scattering is equal to v. The number of neutrons (N_0) passing through an area dS per second after scattering is:

$$\mathrm{N}_0 = v dS |\psi_{scat}|^2 = \frac{v dS b^2}{r^2} = v b^2 d\Omega \qquad (6)$$

The number of incident neutrons passing through a unit area

$\Phi = v|\psi_0|^2 = v$, therefore:

$$\frac{d\sigma}{d\Omega} = \frac{vb^2 d\Omega}{\Phi d\Omega} = b^2 \qquad (7)$$

and the total scattering cross section is determined by the following equation:

$$\sigma_{total} = 4\pi b^2 \qquad (8)$$

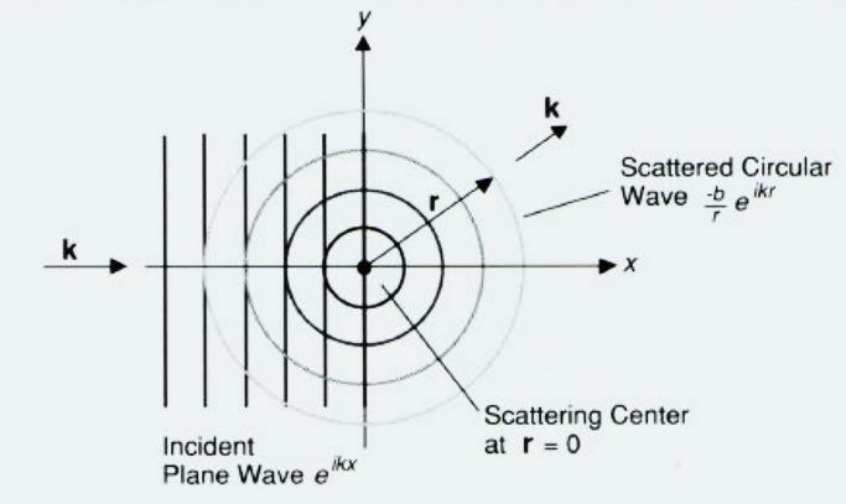

Fig. 2. Scattering of a neutron by a fixed atom.

However, condensed matter contains many atoms, so it is necessary to take into account the scattering of neutrons by these atoms. Let the radius vector $\vec{R}_i$ determine the position of the atoms. The incident neutron is described by wave function $\psi_0 = e^{ik_0\vec{R}_i}$. Scattered neutron will be described by wave function:

$$\psi_{scat} = \sum e^{i\overrightarrow{k_0}\vec{R}_i}\left[\frac{-b_i}{|\vec{r}-\vec{R}_i|} e^{i\vec{k}'(\vec{r}-\vec{R}_i)}\right] \qquad (9)$$

Then differential scattering cross section (from equations 2 and 6) has following form:

$$\frac{d\sigma}{d\Omega} = \frac{vdS|\psi_{scat}|^2}{vd\Omega} = \frac{dS}{d\Omega}\left|b_i e^{i\vec{k}'\vec{r}} \sum \frac{1}{|\vec{r}-\vec{R}_i|} e^{i(\overrightarrow{k_0}-\vec{k}')\vec{R}_i}\right| \qquad (10)$$

If measurements take place at large distances (r >> R_i), then equation (10), taking into account $d\Omega = \mathrm{dS}/\mathrm{r}^2$, is transformed into the equation:

$$\frac{d\sigma}{d\Omega} = \sum_{i,j} b_i b_j \, e^{i(\overrightarrow{k_0}-\vec{k}')(\vec{R}_i-\vec{R}_j)} = \sum_{i,j} b_i b_j \, e^{-i\vec{Q}(\vec{R}_i-\vec{R}_j)} \qquad (11)$$

In which the vector $\vec{Q}$ is defined according to $\vec{Q} = \vec{k}' - \vec{k}_0$.

The scattering length, b_i depends on nuclear isotope, spin relative to the neutron and nuclear eigenstate. Taking into account the averaging of the vector b_i, equation (11) can be written as:

$$\frac{d\sigma}{d\Omega} = \langle b \rangle^2 \sum_{i,j} e^{-i\vec{Q}(\vec{R}_i - \vec{R}_j)} + (\langle b^2 \rangle - \langle b \rangle^2)N \qquad (12)$$

On the right-hand side of equation (12), the first term describes coherent scattering, and the second term refers to incoherent scattering. The value *N* is number of atoms in scattering system. Thus, total scattering cross section is $\sigma = \sigma_{coh} + \sigma_{inc}$. The σ_{coh} and σ_{inc} values are different for each atom and are collected in Table 1 for some atoms.

Nuclide	$\sigma_{coh}, barn$	$\sigma_{inc}, barn$
^{1}H	1.8	80.2
^{2}H (D)	5.6	2.0
C	5.6	0.0
O	4.2	0.0
Al	1.5	0.0
V	0.02	5.0
Fe	11.5	0.4
Cu	7.5	0.5

Table 1. Values of cross section for coherent and incoherent scattering for some nuclei.

In the case of inelastic scattering, differential scattering cross section will be described by equation (13) for coherent scattering and equation (14) for incoherent scattering:

$$\left(\frac{d^2\sigma}{d\Omega d\mathrm{E}}\right)_{coh} = b_{coh}^2 \frac{k'}{k} NS(\vec{Q}, \omega) \qquad (13)$$

$$\left(\frac{d^2\sigma}{d\Omega d\mathrm{E}}\right)_{inc} = b_{inc}^2 \frac{k'}{k} NS_i(\vec{Q}, \omega) \qquad (14)$$

In which $S(\vec{Q}, \omega) = \frac{1}{2\pi\hbar} \iint G(\overrightarrow{r,t})\, e^{i(\vec{Q}\vec{r} - \omega t)} d\vec{r} dt$

and

$$S_i(\vec{Q}, \omega) = \frac{1}{2\pi\hbar} \iint G_s(\overrightarrow{r,t})\, e^{i(\vec{Q}\vec{r} - \omega t)} d\vec{r} dt$$

In these equations G(r,t) is probability of finding a nucleus at (r,t) given that there is one at r=0 at t=0, G_s(r,t) is probability of finding a nucleus at (r,t) if the same nucleus was at r=0 at t=0. Inelastic coherent scattering measures correlated motions of atoms. Inelastic incoherent scattering measures self-correlations e.g. diffusion.

Obtaining a neutron flux is difficult task. To obtain a powerful flux of neutrons, nuclear reactors are used. At the Joint Institute for Nuclear Research, IBR-2 reactor is used to obtain a neutron flux. In general terms, the reactor is discussed in the next section.

Reactor IBR-2

The IBR-2 reactor is a pulsed fast reactor of periodic action. The reactor has one of the highest neutron fluxes in the world ~10^{16} neutron per cm^2 per sec. The average reactor power is 2 MW. The reactor uses plutonium dioxide (PuO_2) as fuel. The structure of the reactor core is shown in Fig. 3.

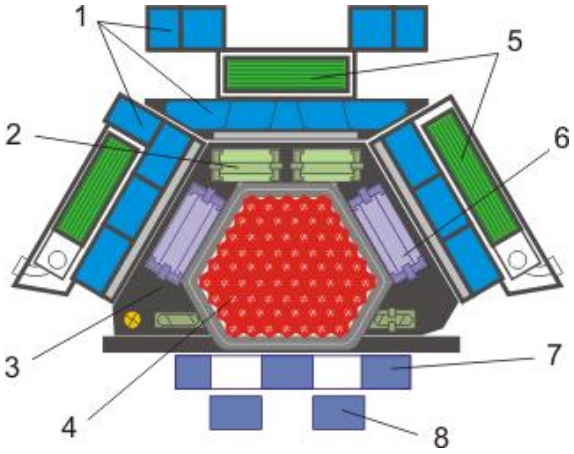

The main components of the reactor:

1 - Water moderators
2 - Safety system
3 - Stationary reflector
4 - Fuel assemblies
5 - Cold moderators
6 - Control rods
7 - Main movable reflector
8 - Auxiliary movable reflector

Fig. 3. Schematic depiction of IBR-2 reactor core (scheme taken from http://flnph.jinr.ru/en/facilities/ibr-2/parameters).

The main difference from other reactors is mechanical modulation of reactivity using a movable reflector made of an alloy of nickel and steel. The movable reflector consists of a main movable reflector 7 and an auxiliary movable reflector 8, which rotate in opposite directions at different speeds. A pulse is generated when both reflectors are aligned. Scientific researches are carried out using neutron beams extracted from the reactor.

NERA Spectrometer

NERA spectrometer was used to record the spectra of inelastic incoherent scattering of the compound of our choice. This spectrometer is installed at a distance of 100 m from the water moderators at the end of neutron guide. This spectrometer belongs to reverse geometry spectrometers and is used primarily for studying molecular dynamics. The sample environment system allows one to obtain the results of experiments of inelastic scattering and diffraction at low temperatures (from 5 to 300 K) and high pressure (up to 400 MPa). The energy of incident neutron is determined by the time of flight of neutron from the moderator to the detector and measurement of neutron energy after scattering. The main components of NERA spectrometer are shown schematically in Figure 4.

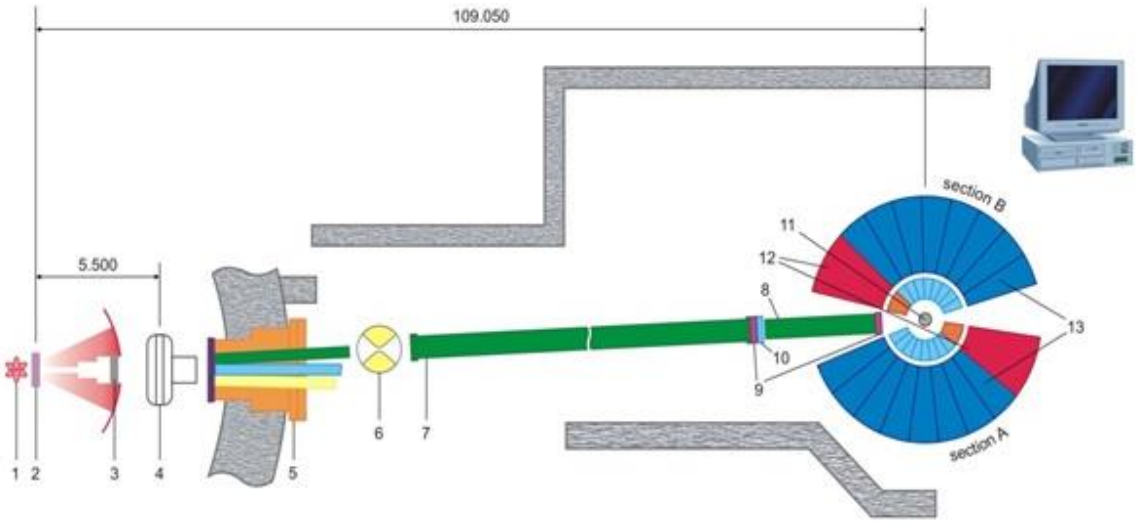

1 – IBR-2 reactor core
2 – Thermal and cold moderators of radial horizontal beamlines 7-11 and tangential beamlines 1–9
3 – Beam shutter
4 – Fast neutron background chopper
5 – Common vacuum splitter of three neutron beams by Ni-mirror neutron guides
6 – l-chopper of beamline 7b
7 –Vacuum Ni-mirror guide tube of neutron beamline 7b
8 – Vacuum sections of beamline 7b
9-10 – Monitor and diaphragms of incident beam 7b, respectively
11 – Sample position
12 – NPD sections
13 – INS and QENS sections of the NERA spectrometer.
13 – Section INS и QENS of NERA

Fig. 4. Main components of NERA spectrometer (scheme taken from http://flnph.jinr.ru/en/facilities/ibr-2/instruments/nera).

The neutron beam leaves IBR-2 reactor core (1) and slows down on thermal and cold moderators (2), then the background of fast neutrons is removed (4). The neutron beam then passes through vacuum beam splitter (5) and beam chopper (6). The resulting neutron flux is directed through neutron tube (7), monitor and diaphragms (9-10) to the sample (11).

The detector consists of two identical sections (Fig. 5).

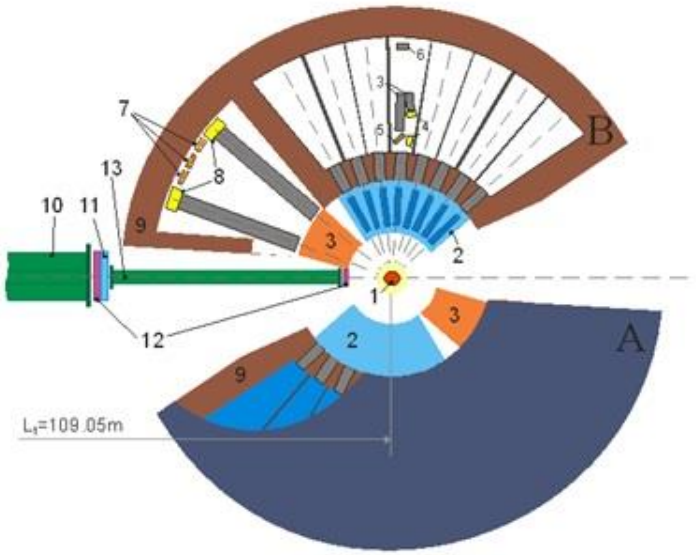

1 – Sample
2 – Be-filters
3 – Collimators
4 – ^{3}He detectors (INS and QNS)
5 – PG analyzers (INS)
6 – Single crystal analyzers (QNS)
7 – Detectors for high intensity diffraction
8 – Diffraction detectors with good collimation
9 – Spectrometer shielding
10 – Ni-coated mirror neutron guide in a vacuum tube
11-12 – Diaphragms and monitor of incident beam 7b, respectively
13 – Vacuum neutron guide.

Fig. 5. The main components of detector of NERA spectrometer (scheme taken from http://flnph.jinr.ru/en/facilities/ibr-2/instruments/nera).

In the detector, the neutron flux from the source enters the sample through neutron guide, diaphragms and monitor (10-13). The neutron beam scattered on the sample (1) passes through Be-filters, a set of detectors and collimators (3-4). This design provides monochromaticity of scattered neutron beam and allows register energies and angles of neutron scattering.

Fig. 6. General view of NERA spectrometer detector (image taken from http://flnph.jinr.ru/en/facilities/ibr-2/instruments/nera).

The spectrometer detects neutrons with energies up to 130 meV. The inelastic incoherent scattering spectra presented in results section were obtained using NERA spectrometer.

Application of IINS for hydrogen bond research

Inelastic incoherent neutron scattering is an individual form of vibrational spectroscopy. As mentioned above, this type of spectroscopy, together with Raman spectroscopy and IR spectroscopy, provide the most complete information about atoms and molecules vibrations in materials.

Hydrogen bond formation can be traced from IINS spectra. The most informative are hydrogen atom vibrations involved in the formation of hydrogen bonds. The formation of hydrogen bond leads to the change in the vibration frequency. Figure 7 shows an example of vibrations for the most common hydrogen bonds type of OHO: stretching vibration ν(O–H), deformation vibration δ (deformation of R–O–H angle) and γ (deformation of R–O–H angle relative to R–O bond).

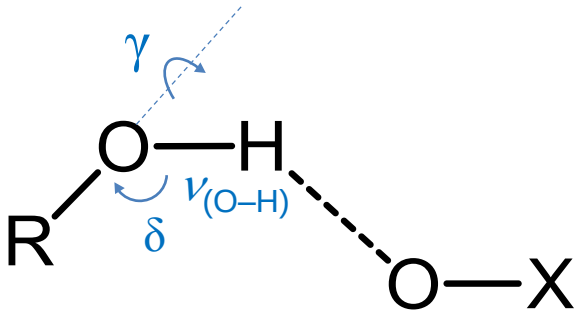

Fig. 7. The characteristic vibrations of atoms in hydrogen bond are observed in the IINS spectra.

The typical value of stretching vibration frequency for the case of hydrogen bond absence is 3200 cm^{-1}. After formation of hydrogen bond, it shifts to about 2900 cm^{-1}. Vibration of δ (about 500 cm^{-1} in the absence of hydrogen bond) becomes difficult and deformation in hydrogen bond plane (the plane formed by O–H···O atoms) with frequency value from 900 cm^{-1} to 1500 cm^{-1}. Vibration of γ transforms into out-of-plane deformation and is observed in the range from 600 cm^{-1} to 1200 cm^{-1}. By analyzing the IINS spectra, it is possible to detect the formation of hydrogen bond by changing these frequencies.

Bilirubin

We investigated hydrogen bond in bilirubin (Fig. 8).

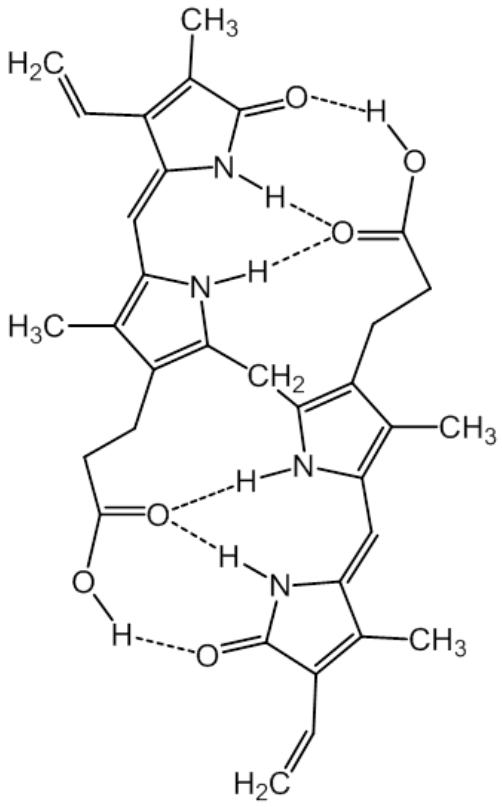

Fig. 8. The structure of bilirubin molecule. Dashed lines indicate hydrogen bonds.

As a result of the destruction of old or abnormal red blood cells, waste products appear in organism, which are then excreted. During the catalytic process, biliverdin is produced from heme (a substance needed to bind oxygen in the bloodstream). Then bilirubin is produced from biliverdin. Bilirubin metabolites are excreted in the urine and bile. An increased level of bilirubin in the bloodstream may indicate presence of diseases for example hemolytic jaundice, hepatic jaundice, blockage of bile ducts and others. In the blood, bilirubin is contained in two fractions: bound and unbound. Unbound bilirubin, unlike bound bilirubin, is quite toxic, able to easily penetrate cells and disrupt their functions. Therefore, indicators of total, bound and unbound bilirubin in the bloodstream are used to accurately diagnose the disease.

Bilirubin is insoluble in water and most polar solvents, including diethyl ether, ethanol. It is highly soluble in non-polar solvents.

Our work, carried out during the summer student program, is devoted to the study of intramolecular hydrogen bonds vibrations in bilirubin using spectroscopy methods and quantum chemistry calculations.

Results

In bilirubin there are several proton-donor groups O–H and N–H, and proton-acceptor groups C = O. Therefore, the formation of intramolecular hydrogen bonds of type O–H···O and N–H···O is possible (Fig. 8).

To obtain the most complete information about the vibrations in bilirubin, we used three spectroscopic methods: IR, Raman, and IINS.

IR and Raman spectra were recorded for solid state using a Bruker IFS 66 FT-IR and Nicolet Magna 860 FT-Raman spectrometers.

IINS spectra were recorded at the Joint Institute for Nuclear Research using a time-of-flight spectrometer NERA with reverse geometry. IBR-2 reactor was used as a neutron source. The spectrum recording temperature was 10K.

Additionally, quantum-chemical calculations of geometry (Fig. 9) of bilirubin in the gas phase and vibration frequencies were performed. The DFT method was used for calculations of geometry. All calculations were performed using Gaussian 16 program [25]. To obtain optimized geometry, we used B3LYP functional and 6-31+G(d, p) basis set. This combination is often used to calculate geometry of hydrogen bonded compounds [26].

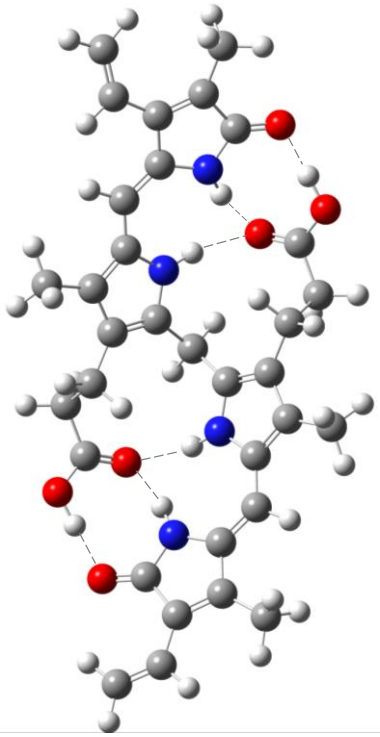

Fig. 9. Optimized geometry of bilirubin molecule obtained using quantum chemical calculations. Hydrogen bonds are indicated by dotted lines.

Bilirubin contains O–H···O and N–H···O hydrogen bonds. In the second case, two N–H groups are bonded to one oxygen atom. The types of atomic vibrations in hydrogen bond are shown schematically in Scheme 1 and Scheme 2.

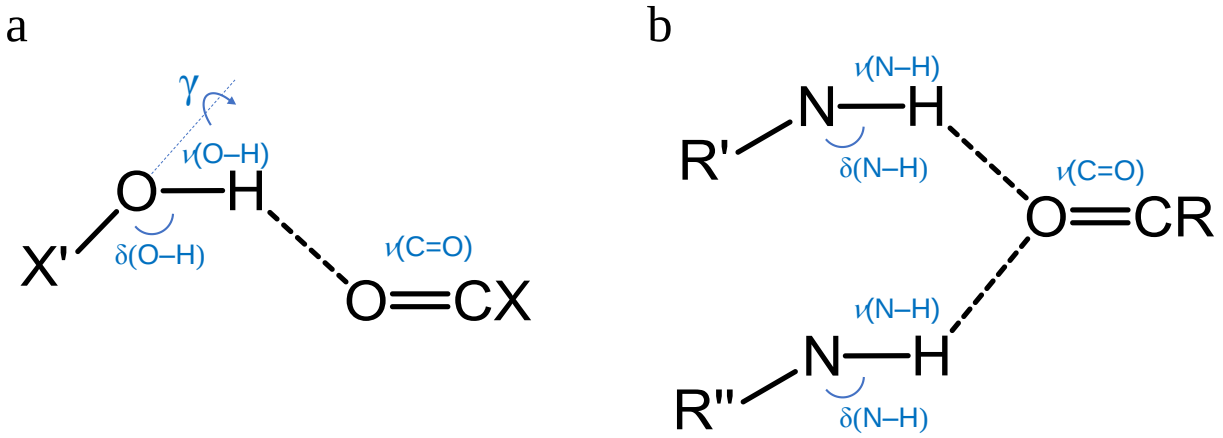

Scheme 1. Types of atomic vibrations in O–H···O hydrogen bond (a) and N–H···O hydrogen bond (b). Out of plane deformations in N–H···O hydrogen bond are shown in Scheme 2.

Hydrogen bond O–H···O has stretching vibration ν(O–H), deformation of bond angle δ(O–H), and out-of-plane deformation γ(O–H) (Scheme 1a). In N–H···O hydrogen bond, there are two stretching vibrations ν(N–H), deformations of bond angles δ(N–H) (Scheme 1b), and two types of out-of-plane deformation γ_s(N–H) (Scheme 2a) and γ_{as}(N–H) (Scheme 2b). In the case of γ_s(N–H) deformation hydrogen atoms move in one direction outside the plane, and in the case of γ_{as}(N–H) deformation they move in different directions outside the plane.

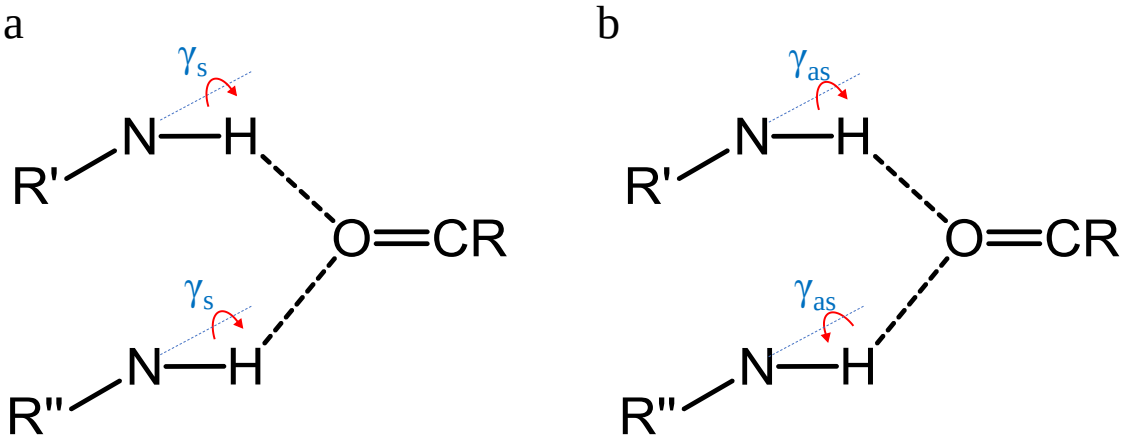

Scheme 2. Symmetrical (a) and asymmetrical (b) out of plane deformations in N–H···O hydrogen bond.

In Fig. 10 shows IR spectra in the range from 400 cm^{-1} to 3750 cm^{-1}. The assignment of signals in spectrum was performed using frequencies obtained by DFT calculations. The spectrum shows intense stretching vibrations ν(N–H) = 3411 cm^{-1}, ν(N–H) = 3262 cm^{-1} and ν(O–H) = 2500 cm^{-1}. The band with frequency equal to 1690 cm^{-1} was assigned to C=O group stretching vibration. This band is the most intense in spectra. In the region of 400 – 1700 cm^{-1}, deformation vibrations are observed. For hydrogen bond in bilirubin, these are deformations of C–O–H and C–N–H angles in hydrogen bond plane (Scheme 2), and out-of-plane deformation of hydrogen atom (Scheme 1 and Scheme 2).

Deformation vibrations δ(N–H) and δ(O–H) in hydrogen bond plane are observed at frequency ~1610 cm^{-1}. The bands with frequencies γ(O–H) = 924 cm^{-1} and γ_s(N–H) = 699 cm^{-1} were assigned to out-of-plane deformation in hydrogen bonds of O–H···O and N–H···O types, respectively.

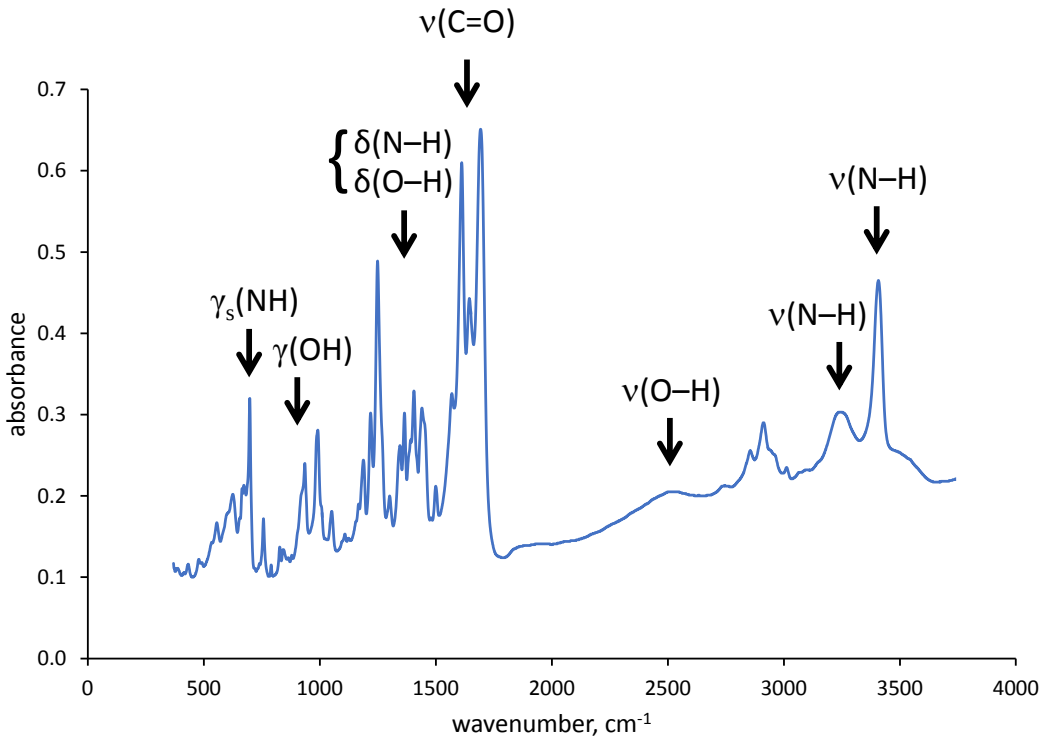

Fig. 10. IR spectra of bilirubin. Signal assignment is performed using calculated frequencies.

Deformation vibrations are also observed in Raman spectra (Fig. 11). The assignment of signals in spectrum was performed using frequencies obtained by DFT calculations. However, the vibrations δ(N–H) and δ(O–H) are less have a lower relative intensity in comparison with intensity in IR spectra. Signal assignment is performed using calculated frequencies.

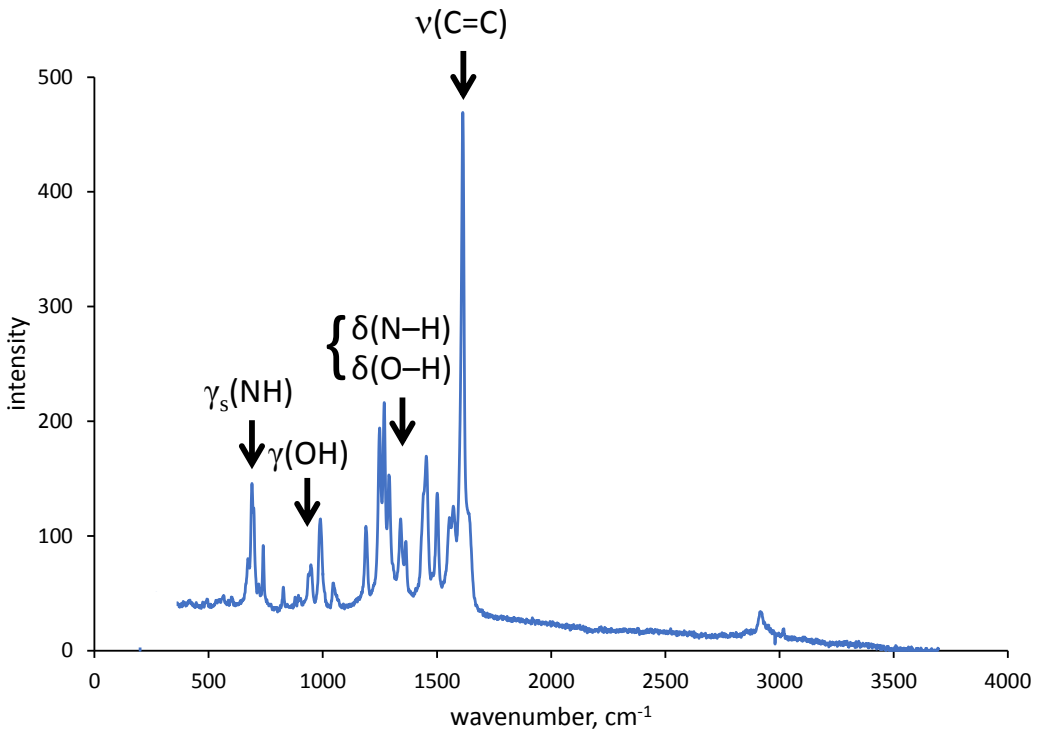

Fig. 11. Spectra of bilirubin recorded by Raman spectroscopy. Signal assignment is performed using calculated frequencies.

At the Joint Institute for Nuclear Research, the spectra of inelastic incoherent neutron scattering (Fig. 12) in bilirubin powder were recorded. The spectra were recorded using a NERA spectrometer.

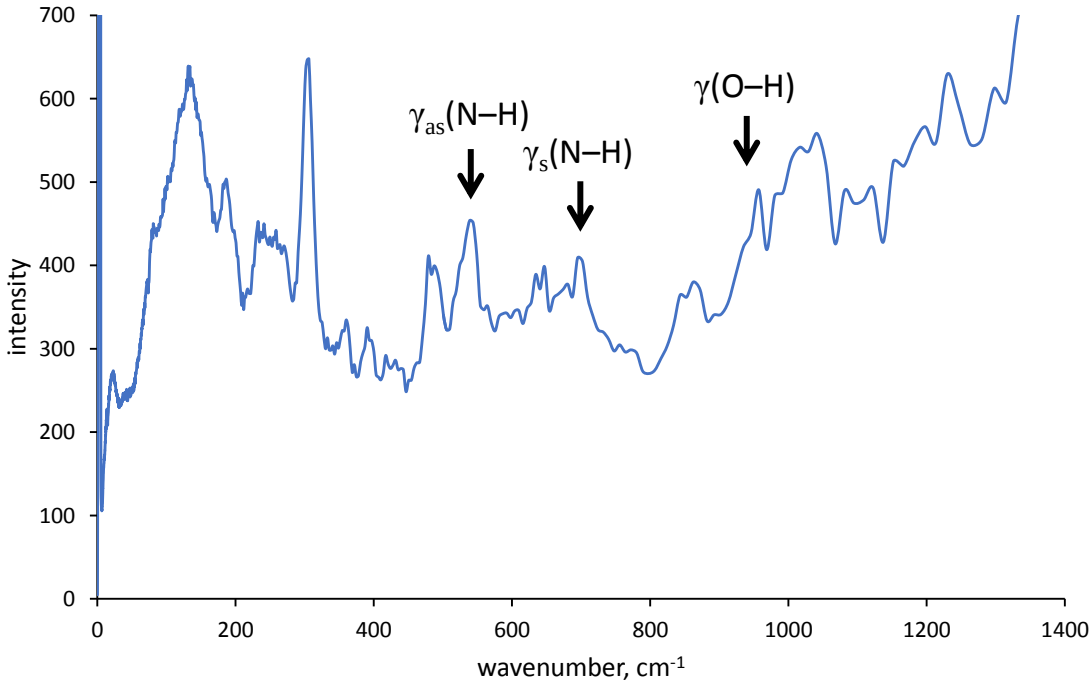

Fig. 12. IINS spectra of bilirubin recorded at 10 K using NERA time-of-flight spectrometer with reverse geometry, included in scientific and technical equipment of JINR.

Using these spectra it is possible to study low-frequency vibrations in bilirubin. Signal assignment performed using DFT calculations. In this

region, deformation vibrations are observed, which are related to out-of-plane deformation in hydrogen bond γ(O–H) = 945 cm^{-1} for O–H···O hydrogen bond. For N–H···O hydrogen bond, two out-of-plane deformations are observed: symmetric (the case when both protons leave plane in one direction) and asymmetric (the case when protons leave plane on opposite sides). Asymmetric deformation γ_{as}(N–H) = 534 cm^{-1} is observed in region of lower frequencies in comparison with symmetric deformation γ_{s}(N–H) = 695 cm^{-1}.

The obtained IINS spectra show bands in low-frequency region that were not seen in IR and Raman spectra.

Summary

Participation in the Summer Student Program provided an opportunity to get acquainted with unique equipment for experiments, learn about their structure and operation, and gain knowledge about neutron scattering during excursions to the laboratory of the Institute.

To study bilirubin, we used method of inelastic incoherent neutron scattering. The high sensitivity of IINS method to hydrogen atoms provides a special interest in this method as applied to investigate of hydrogen bonds. An additional advantage of using IINS method is its high sensitivity to isotopes, which makes it possible to observe isotope substitution effects, for example, H/D isotope effects.

During the Summer Student Program, spectra of inelastic incoherent neutron scattering were obtained and analyzed for bilirubin, the molecule that contains intramolecular hydrogen bonds. The spectra were recorded using time-of-flight spectrometer NERA with reverse geometry. The use of IINS method for the study of hydrogen bonds in conjunction with IR and Raman spectroscopy made it possible to obtain the most complete information about vibrational states in bilirubin.

Acknowledgements

I would like to thank Prof. Dr. Sc. A.I. Filarowski for the opportunity to take part in Summer Student Program, for knowledge about experimental equipment and help and support in work.

I would like to thank my supervisor Prof. Dr. Sc. P.M. Tolstoy for help in preparing for Summer Student Program and for support during my stay in Dubna.

I would also like to thank Dr. E.A. Goremychkin for measuring IINS spectra using NERA spectrometer.

Referencies

[1] F. Manzenrieder, A. Frank, H. Kess, *Angew. Chem. Int. Ed.*, **2008**, 47, 2608
[2] J. Mavri, H. Vogel, *Proteins*, **1996**, 24, 495
[3] K. Manikandan, S. Ramakumar, *Pub. Med.*, **2004**, 56, 768
[4] C. Jones, P. Baruah, A. Thompson, S. Scheiner, M. Smith, *J. Am. Chem. Soc.*, **2012**, 134, 12064
[5] T. Tiekink, J. Zukerman-Schpector, M. Nishio, Y. Umezawa, H. Suezawa, *Chem. Commun.*, **2011**, 47, 6623-6625
[6] R. Benesch, R. Benesch, *Adv. Protein Chem.*, **1974**, 28, 211
[7] K. Opper, B. Fassbender, G. Brunklaus, H. Spiess, K. Wagener, *Macromolecules*, **2009**, 42, 4407
[8] E. Arunan, G. Desiraju, R. Klein3, J. Sadlej, S. Scheiner, I. Alkorta, D. Clary, R. Crabtree, J. Dannenberg, P. Hobza, H. Kjaergaard, A. Legon, B. Mennucci, D. Nesbitt, *Pure Appl. Chem.*, **2011**, 83, 8, 1637–1641.
[9] S. Kucherov, S. Bureiko, G. Denisov, *J. Mol. Struct.*, **2016**, 1105, 246–255.
[10] P. Tolstoy, P. Schah-Mohammedi, S. Smirnov, N. Golubev, G. Denisov, H. Limbach, J. *Am. Chem. Soc.*, **2004**, 126, 5621
[11] B. Koeppe, P. Tolstoy, H. Limbach, *J. Am. Chem. Soc.*, **2011**, 133, 7897
[12] I. Shenderovich, P. Tolstoy, N. Golubev, S. Smirnov, G. Denisov, H. Limbach, *J. Am. Chem. Soc.*, **2003**, 125, 11710–11720.
[13] R. Marek, A. Lycka, E. Kolehmainen, E. Sievanen, J. Tousek, *Curr. Org. Chem.*, **2007**, 11, 1154–1205
[14] A. Silva, X. Kong, R. Hider, *BioMetals*, **2009**, 22, 771–778.
[15] S. Grabowski, *J. Phys. Org. Chem.*, **2004**, 17, 18–31.
[16] E. Lippincott, R. Schroeder, *J. Chem. Phys.*, **1955**, 23, 1099–1106.
[17] R. Schroeder, E. Lippincott, *J. Phys. Chem.*, **1957**, 61, 921–928.
[18] A. Iogansen, *Spectrochim. Acta - Part A Mol. Biomol. Spectrosc.*, **1999**, 55, 1585–1612.
[19] W. Mikenda, *J. Mol. Struct.*, **1986**, 147, 1–15.
[20] M. Hippler, S. Hesse, M. Suhm, *Phys. Chem. Chem. Phys.*, **2010**, 12, 13555–13565
[21] T. Brückel, G. Heger, D. Richter, G. Roth, R. Zorn (Editors), Jülich Centre For Neutron Science (JCNS), "Neutron Scattering".
[22] P. Mitchell, S. Parker, A. Ramirez-Cuesta, J. Tomkinson, "Vibrational Spectroscopy with Neutrons, with Applications inChemistry, Biology, Materials Science and Catalysis", *World Scientific: Singapore*, **2005**.
[23]Ł. Hetmańczyk, P. Szklarz, A. Kwocz, M. Wierzejewska, M. Pagacz-Kostrzewa, M. Melnikov, P. Tolstoy, A. Filarowski, *Molecules*, **2021**, *26*(11), 3109.
[24] R. Pynn, *Los Alamos National Laboratory*, "Neutron scattering".
[25] M. J. Frisch, G. W. Trucks, H. B. Schlegel, G. E. Scuseria, M. A. Robb, J. R. Cheeseman, G. Scalmani, V. Barone, G. A. Petersson, H. Nakatsuji, M. C. X. Li, A. V. Marenich, J. Bloino, B. G. Janesko, R. Gomperts, B. Mennucci, H. P. Hratchian, J. V. Ortiz, A. F. Izmaylov, J. L. Sonnenberg, D. Williams-Young, F. Ding, F. Lipparini, F. Egidi, J. Goings, B. Peng, A. Petrone, T. Henderson, D. Ranasinghe, V. G. Zakrzewski, J. Gao, N. Rega, G. Zheng, W. Liang, M. Hada, M. Ehara, K. Toyota, R. Fukuda, J. Hasegawa, M. Ishida, T. Nakajima, Y. Honda, O. Kitao, H. Nakai, T. Vreven, K. Throssell, J. A. Montgomery, J. E. P. Jr., F. Ogliaro, M. J. Bearpark, J. J. Heyd, E. N. Brothers, K. N. Kudin, V. N. Staroverov, T. A. Keith, R. Kobayashi, J. Normand, K. Raghavachari, A. P. Rendell, J. C. Burant, S. S. Iyengar, J. Tomasi, M. Cossi, J. M. Millam, M. Klene, C. Adamo, R. Cammi, J. W. Ochterski, R. L. Martin, K. Morokuma, O. Farkas, J. B. Foresman and D. J. Fox, Gaussian, Inc., Wallingford CT, 2016.
[26] J. Ireta, J. Neugebauer, M. Scheffler, *J. Phys. Chem. A*, **2004**, 108, 5692-5698